

A Cranial Base of *Australopithecus robustus* from the Hanging Remnant of Swartkrans, South Africa

Darryl J. de Ruiter,^{1*} Christine M. Steininger,² and Lee R. Berger²

¹Department of Anthropology, Texas A&M University, College Station, Texas 77843

²School of Geosciences, University of the Witwatersrand, Johannesburg 2050, South Africa

KEY WORDS SKW 18; *Australopithecus robustus*; cranial base anatomy; variation; dimorphism

ABSTRACT SKW 18, a partial hominin cranium recovered from the site of Swartkrans, South Africa, in 1968 is described. It is derived from ex situ breccia of the Hanging Remnant of Member 1, dated to approximately 1.5–1.8 Mya. Although partially encased in breccia, it was refit to the facial fragment SK 52 (Clarke [1977] The Cranium of the Swartkrans Hominid SK 847 and Its Relevance to Human Origins, Ph.D. dissertation, University of the Witwatersrand, Johannesburg), producing the composite cranium SKW 18/SK 52. Subsequent preparation revealed the most complete cranial base attributable to the species *Australopithecus robustus*. SKW 18 suffered weathering and slight postdepositional distortion, but retains considerable anatomical detail. The composite cranium most likely represents a

large, subadult male, based on the incomplete fusion of the sphenoccipital synchondrosis; unerupted third molar; pronounced development of muscular insertions; and large teeth. Cranial base measures of SKW 18 expand the range of values previously recorded for *A. robustus*. SKW 18 provides information on anatomical features not previously visible in this taxon, and expands our knowledge of morphological variability recognizable in the cranial base. Morphological heterogeneity in the development of the prevertebral and nuchal muscular insertions is likely the result of sexual dimorphism in *A. robustus*, while differences in cranial base angles and the development of the occipital/marginal sinus drainage system cannot be attributed to size dimorphism. *Am J Phys Anthropol* 130:435–444, 2006. © 2006 Wiley-Liss, Inc.

Hominid remains attributed to *Australopithecus robustus* have been recovered from six localities in South Africa: Kromdraai (Broom, 1938), Swartkrans (Broom, 1949), Drimolen (Keyser et al., 2000), Gondolin (Menter et al., 1999), Sterkfontein (Kuman and Clarke, 2000), and Coopers (Berger et al., 2003). The majority are derived from the site of Swartkrans (Brain, 1981; Oakley, 1977). Although almost 500 fossils have been referred to this taxon, specimens preserving the cranial base are rare (Brain, 1981; Broom and Robinson, 1952; Grine, 1993; Grine and Strait, 1994). What cranial base remains have been recovered tend to be either highly fragmentary or badly damaged/distorted, and even superbly complete specimens such as DHN 7 are deficient in this region (Keyser, 2000). Discussion of cranial base morphology in *A. robustus* is therefore constrained to a limited range of anatomical regions, typically involving small numbers of specimens or individual fossils (Falk, 1986a; McKee and Helman, 1991; Olson, 1978, 1981; Rak and Clarke, 1979; Tobias, 1967; Tobias and Symons, 1992). As such, little is known regarding intraspecific variability in the cranial base within this taxon, and whole anatomical areas are entirely unknown. The recovery of additional cranial base materials is therefore of significance for our understanding of morphological variability in this poorly known anatomical region of *A. robustus*.

SKW 18 is a relatively complete cranial base specimen recovered in 1968 by C.K. Brain from ex situ Member 1, Hanging Remnant breccia dumps, dated to approximately 1.5–1.8 Mya (Brain, 1993; Curnoe et al., 2001; de Ruiter, 2003; Vrba, 1985). Clarke (1977) first recognized that SKW 18 could be refit to SK 52, a partial facial fragment recovered in 1949 (Broom and Robinson, 1952). The two specimens present clear points of contact in the

mastoid and tympanic regions; the remainder of the refit (i.e., the facial region) is considerably more fragmented (Fig. 1). Clarke (1977, p. 256) cleaned a portion of the cranial base of SKW 18, and provided a preliminary description of the nuchal and occipitomastoid regions. However, it remained mostly encased in breccia until 2000, when one of us (D.J.d.R.) prepared it out via immersion in 10% acetic acid, using a protocol similar to that developed by Brain (personal communication) at Swartkrans.

The pattern of dental eruption in SK 52 indicates an age of about 15 years (± 3 years) according to human standards (Mann, 1975; Ubelaker, 1989), or between 7–8 years of age according to chimpanzee standards (Conroy and Kuykendall, 1995). The sphenoccipital synchondrosis fuses in 95% of humans between ages 20–25 years (Krogman and İşcan, 1986); thus, the unfused nature of this cranial feature in SKW 18 indicates that it is probably younger than 20 years of age, consistent with the

Grant sponsor: Palaeo-Anthropology Scientific Trust; Grant sponsor: National Research Foundation, South Africa; Grant sponsor: Conservation Corporation of Africa; Grant sponsor: Texas A&M International Research Travel Assistance Grant.

*Correspondence to: Darryl de Ruiter, Department of Anthropology, Texas A&M University, College Station, TX 77843-4352. E-mail: deRuiter@tamu.edu

Received 8 April 2005; accepted 18 October 2005.

DOI 10.1002/ajpa.20386

Published online 19 January 2006 in Wiley InterScience (www.interscience.wiley.com).



Fig. 1. SKW 18 conjoined with SK 52 to form composite cranium. **A:** Right lateral aspect. **B:** Superior aspect. Note that SK 52 temporal fragment in **B** does not align perfectly as a result of damage, though the refit is considered reliable. Scale bar is 50 mm.

dental age estimate of SK 52. The powerful development of the mastoid processes and muscle markings of SKW 18 suggest a male individual. Odontometrically, SK 52 represents one of the largest individuals in the *A. robustus* hypodigm (Robinson, 1956). It is therefore concluded that the composite cranium SKW 18/SK 52 is most likely that of a large, subadult male (see also Oakley, 1977).

This paper presents a comprehensive description and comparative analysis of SKW 18, the most complete cranial base known from *A. robustus*. Anatomical terminology follows Weidenreich (1943), Tobias (1967), and *Terminologia Anatomica* (Federative Committee on Anatomical Terminology, 1998). Observations were aided by a binocular microscope where possible. All dimensions are chord distances, and values are reported in millimeters, recorded to the nearest 0.1.

DESCRIPTION

Preservation

SKW 18 was moderately weathered, and is pervaded by numerous small cracks (Figs. 2, 3). Several flakes of the inner bone table became loosened in both the middle and posterior cranial fossae, and a large section of the inner

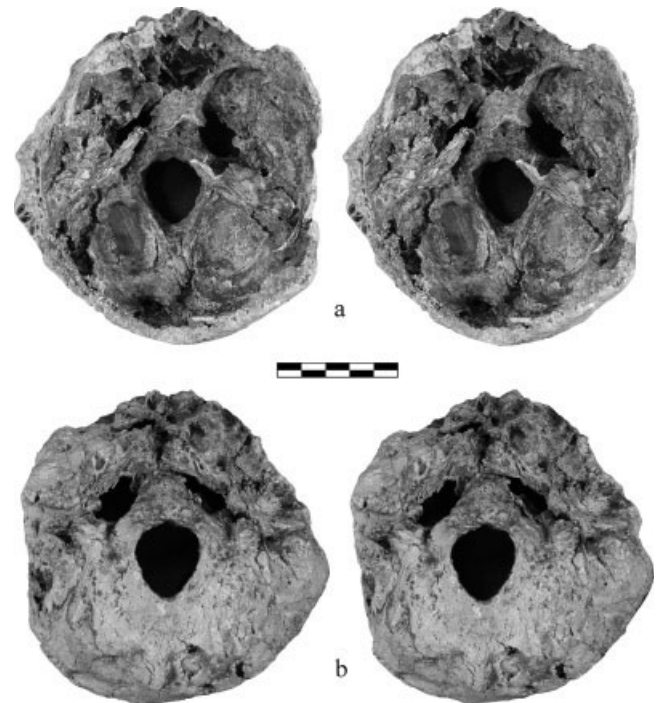


Fig. 2. SKW 18 in stereo view. **A:** Superior aspect. **B:** Inferior aspect. Plastic deformation is evident in left preglenoid area, as well as in slight lateral displacement of basioccipital.

bone table is missing superior to the transverse limbs of the cruciform eminence. During preparation of the specimen, numerous freed bone flakes were recovered from out of anatomical position in the breccia, indicating that they became loosened prior to excavation. Small pools of breccia remain in the very bottom of the cerebellar fossae. The calvaria is missing, having been broken away approximately 40.0 above the petrous part on the right side; on the left, the calvaria was removed approximately 23.0 above the petrous part anteriorly, angling down to about 5.0 below the petrous part posteriorly. The facial skeleton (SK 52) was obliquely sheared off immediately anterior to the middle cranial fossa. Viewed from the posterior aspect, the cranium presents a broad, squat profile truncated by damage to the lateral extent of both sides. The left mastoid area is still preserved, while the right was broken away along with most of the temporal squama, leaving behind a thin veneer of the inner bone table and producing a skewed posterior contour. Part of the damaged right temporal is preserved in SK 52. The entire nuchal area was moderately weathered, and there is a large area of cortical damage to the left of the external occipital protuberance. Although this cranium was widely damaged, plastic deformation appears minimal. The most extensively deformed aspect is the preglenoid region of the left side of the cranium anterior to the mandibular fossa, which was displaced posteromedially (Figs. 2b, 3c). The foramen magnum was slightly distorted as a result of lateral displacement of the basioccipital (Fig. 2b).

Internal aspect of SKW 18

Small fragments of the sphenoid, ethmoid, and vomer are preserved in what remains of the anterior cranial fossa, held together in a mass of breccia and glue (Fig. 2a). Although the ethmoid was almost entirely

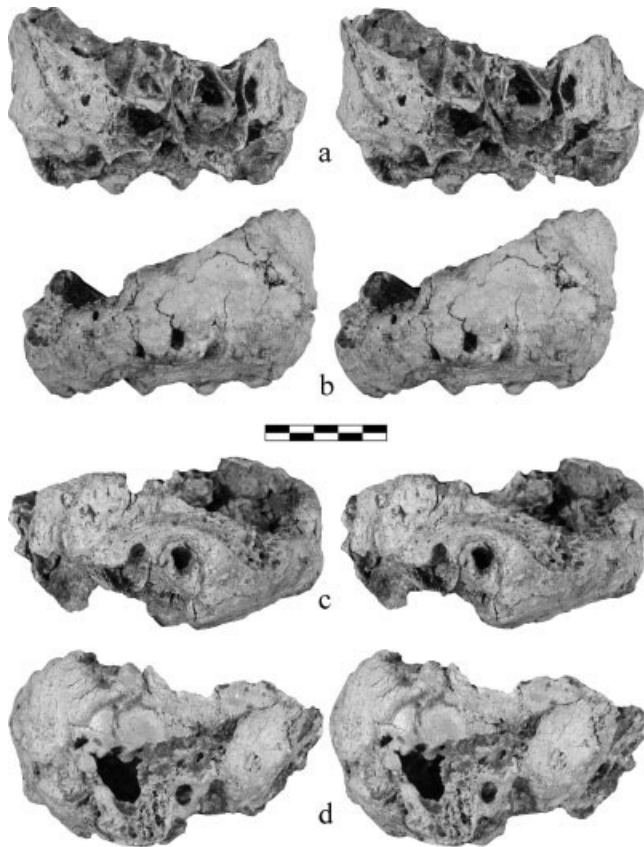


Fig. 3. SKW 18 in stereo view. **A:** Anterior aspect. **B:** Posterior aspect. **C:** Left lateral aspect. **D:** Right lateral aspect (note area of conjoint with SK 52 in mastoid/tympanic region). Scale bar is 50 mm.

removed, moderately large ethmoidal air cells can still be traced. Most of the body of the sphenoid anterior to the sella turcica was broken away, revealing well-developed sphenoidal air cells. Bilaterally, much of the lesser wings of the sphenoid are present, sweeping away from the broken body of the sphenoid toward the lateral walls of the cranium. The posterior edges of the lesser wings are bluntly rounded, and do not overhang the middle cranial fossa. No trace remains of the anterior clinoid processes.

In the middle cranial fossa, the well-preserved sella turcica is moderately deep and broad; it broke away from both the left greater wing of the sphenoid and from the basilar occipital, and is shifted approximately 3.0 to the right. The tuberculum sellae was damaged, but part of a weak, left, middle clinoid process is still visible. There is a small, circular foramen at the anterior extent of the floor of the hypophysial fossa. The dorsum sellae is narrow, measuring approximately 13.5 across, and is particularly thin and fragile. It has a marked concave curvature when viewed superiorly, and notably overhangs the hypophysial fossa. Two ridges join the floor of the hypophysial fossa to the posterior clinoid processes. The left posterior clinoid process is missing, but the right is preserved as a very small, anteriorly projecting knob. This remaining posterior clinoid process is unusual in that the process itself is recessed inward (medially) from the lateral extent of the dorsum sellae.

The left carotid sulcus was broken through its longitudinal midline via an approximately 3.0 wide crack, separating the body of the sphenoid from the greater wing of



Fig. 4. Stereo view of broken right petrous, showing middle-ear structures in cross section, view from anterior toward posterior aspect. ma, mastoid antrum; tt, tensor tympani origin; ic, internal carotid canal; tn, tympanic nerve; p, promontory; fc, fenestra cochlea; fv, fenestra vestibuli. Scale bar is 50 mm.

the sphenoid. The right carotid sulcus was slightly distorted by lateral displacement of the sella turcica. The carotid sulci are positioned closely adjacent to the tuberculum sellae, presenting beveled anteromedial borders and bluntly rounded lateral margins. The right sulcus possesses a posteriorly projecting lingula. Although obscured by breccia, the bilaterally preserved superior orbital fissures appear as elongated, narrow channels, separated from the foramen rotundum by a narrow bridge of bone. The foramen rotundum is moderately large and oval-shaped. The foramen ovale is represented by a small, slightly rounded canal completely encircled by the greater wing of the sphenoid. The foramina rotundum and ovale are widely spaced from each other, being 10.9 apart on the left, and 11.5 on the right. On the right side, a short groove for the common trunk of the middle meningeal artery runs laterally and slightly posteriorly from the probable position of the damaged foramen spinosum, until its course is truncated by damage. On the left side, damage partially obliterates the path of the posterior branch of the middle meningeal artery, though a deeply incised groove demarcates its course as it traverses posterosuperiorly along the temporal squama. A weak superior petrosal sulcus is evident bilaterally, though the contact with the sigmoid sinus groove is obscured. A distinct groove, probably for the superior tympanic artery, is visible on the anterior surface of the left petrous part, branching anteriorly from the posterior branch of the middle meningeal artery.

The petrous parts incline forward at approximately 40° to the coronal midline of the specimen. The damaged left petrous part was shifted out of position; it is estimated that the anterior surface was approximately horizontal. The tegmen tympani bulges slightly to accommodate the mastoid antrum. The low, rounded arcuate eminence is notably elongated, coursing almost parallel to the lateral wall of the cranium for approximately 9.0. Although damaged, a shallow trigeminal impression is visible near the apex of the left petrous part. The right petrous part is broken, such that the internal structures can be examined in cross section (Fig. 4). The oval window (fenestra vestibuli) and round window (fenestra cochleae) are visible, separated by a large and inflated promontory similar to other *A. robustus* specimens (Rak and Clarke, 1979). A shallow groove for the tympanic nerve is visible coursing across the promontory. The aditus to the mastoid antrum is in direct contact with the mastoid air cells, the latter evincing considerable pneumatization. The bony canal providing the origin of the m. tensor tympani is positioned adjacent to the internal carotid canal, and immediately superior to the promontory. Laterally, the path of the internal carotid canal can

be followed for approximately 13.0, tracing an almost 90° curve through the petrous part.

Although damaged, the widest breadth of the posterior cranial fossa can be estimated at ca. 85.0. The superior border of the petrous part is bluntly rounded, with no distinct edge. The posterior surface of the petrous part is almost vertical laterally, becoming slightly more oblique medially in the region of the internal acoustic meatus. The height of the posterior surface of the petrous part is 22.1, measured at the anterosuperior lip of the sigmoid sulcus. The bilaterally preserved internal acoustic meatus is round with beveled anterior, superior, and inferior margins, and a thickened posterior margin overhangs the meatus. Approximately 4.1 below the meatus on the left side is the cochlear canaliculus; ca. 3.0 behind the meatus is a small, round porus representing a damaged subarcuate fossa. The left vestibular canaliculus is positioned roughly 5.7 inferolateral to the meatus. The opening of this latter structure is flanked by two bony margins that meet at a right angle, presenting an inferiorly directed, V-shaped notch. On the right petrous part, a segment of the posterior surface is missing, but the aqueducts for the cochlea and vestibule are still evident. A small breccia-filled porus indicates the subarcuate fossa on this side.

The clivus is short and broad, beginning at the anterior margin of the foramen magnum as a moderately concave plane, flattening somewhat as it approaches the dorsum sellae. The lateral edges of the clivus taper from 37.0 wide at the weakly developed tuberculi jugulare to 20.0 at the sphenoccipital synchondrosis. The sphenoccipital synchondrosis is unfused, and the lateral displacement of the sella turcica left a jagged fissure between the sphenoid and the occipital, revealing moderate pneumatization of the basilar occipital. The clivus was slightly displaced laterally, producing a minor skewing of the foramen magnum. The foramen magnum appears oval in outline, with a length/breadth ratio of 80.1%. The widest breadth is anterior to the coronal midline of the foramen. The anterior margin displays a thin shelf of bone superiorly, flanked by two small fossae, and underlain by a thickened shelf of bone inferiorly. An ectobasionic projection is lacking. The lateral and posterior margins of the foramen magnum are represented by a single shelf of bone roughly the same thickness as the inferior anterior shelf all around.

The position of the damaged internal occipital protuberance is estimated at approximately 27.0 superior to opisthion, at roughly the same level as the external occipital protuberance. The cruciform eminence is complete except for the damaged superior sagittal limb. The broad, rounded inferior sagittal limb begins as a single entity, and then splits into bilateral segments posterosuperior to the foramen magnum, producing a small, slightly hollowed vermiform fossa. These bilateral segments continue on either side of the foramen magnum, presenting as bluntly protuberant borders separating the foramen magnum from the cerebellar fossae. The transverse limbs are low and rounded; the right is situated slightly higher than the left, and is slightly sharper. No clearly defined right or left transverse sinus grooves are present. Immediately lateral to the position of the internal occipital protuberance on the right side, a broad, shallow groove for the occipital sinus is palpable on a slightly displaced fragment of the inner bone table; its inferior course rapidly fades to imperceptibility (not owing to damage). Immediately below the internal occipital

protuberance, a very shallow groove for the left occipital sinus obliquely traverses the inferior sagittal limb approximately 21.0 superior to opisthion. There is no indication of either a left or right marginal sinus groove flanking the foramen magnum.

An approximately 5.3 wide portion of the left sigmoid sinus groove is partially embedded in the base of the posterior face of the petrous part, with a thickened shelf of bone overhanging and contributing to the groove. The origin of the sigmoid sinus, whether from a transverse sinus (as in humans) or a combined petrosquamus/superior petrosal sinus (as in OH 5), is obscured in SKW 18. The sigmoid sinus groove traverses medially along the base of the petrous part toward the foramen magnum, and then makes a sharp (ca. 90°) anterior turn toward the jugular foramen. A low, thickened ridge of occipital bone clearly demarcates the course of the sinus posteriorly, remaining salient for its visible duration until it reaches the jugular foramen. This suggests that if a marginal sinus was present, it most likely drained into the larger sigmoid sinus. The cerebellar fossae are relatively large and deep, being bluntly delineated from the foramen magnum medially, and demarcated from the cerebral fossae by the low, rounded transverse limbs of the cruciform eminence. They produce a notably expanded impression on the internal surface of the occipital bone. Superior to the transverse limbs of the cruciform eminence, the cerebral fossae for the occipital lobes appear to have been moderately large and deep, though not as capacious as the cerebellar lobes.

External aspect of SKW 18

A small segment of the unfused lambdoid suture is visible on the right side, disappearing as a result of abrasion prior to reaching the position of asterion (this point is missing bilaterally) (Figs. 2b, 3). Although damage prevents accurate measurement, the lambdoid suture appears to be very high relative to inion. The nuchal plane is tilted at approximately 30° to the Frankfurt horizontal plane, producing a notably horizontally inclined nuchal area; it is moderately flattened sagittally. Although it is not possible to accurately calculate a measure of the plane of the foramen magnum, it appears to have been roughly horizontal in SKW 18.

The unusually developed external occipital protuberance is represented by a thin, sharp ridge of bone roughly 14.5 long and 3.5 wide at its base, extending at its maximum a full 6.7 from the surface of the occipital. The external occipital crest extends all the way to opisthion as a well-developed, bluntly rounded ridge. It is flanked on either side by shallow, oval depressions for the attachment of *m. rectus capitis posterior minor*. The right inferior nuchal line is only faintly outlined at its origin at the anterior extent of the external occipital protuberance; the left side was extensively damaged. Approximately 11.0 lateral to the external occipital protuberance, the right inferior nuchal line becomes more prominently developed. It courses laterally for a further 16.0 before curving sharply anteriorly for roughly 17.0. At its terminus, the inferior nuchal line forms prominent bony ridges bilaterally, the right side being more protuberant than the left. Narrow, elongated depressions anteromedially subadjacent to the bony ridges of the inferior nuchal line indicate the insertion of *m. rectus capitis posterior major*. Posterolateral to the inferior nuchal line, elongated, crescent-shaped impressions are visible on both sides for the insertion of *m. obliquus capitis*

superior, extending anteriorly toward the condylar fossae. On the right side, immediately posterosuperior to the inferior nuchal line, the *m. semispinalis capitis* insertion is visible as a crescent-shaped fan lateral to the external occipital protuberance; damage obscures its development on the left. Approximately 12.0 to the right of the external occipital protuberance, the superior nuchal line becomes prominent as a rounded bony spur, continuing beyond this as a moderately developed ridge. When the temporal fragment of SK 52 is reattached to SKW 18, the right superior nuchal line continues onto the posterolateral aspect of the mastoid process as a bluntly rounded, robust mastoid crest. The damaged left superior nuchal line is only weakly delineated medially, becoming more prominent as it traverses laterally, continuing onto the posterolateral face of the mastoid as a low, rounded mastoid crest.

Approximately 11.0 superior to the right superior nuchal line is a raised rugosity which closely follows the lambdoid suture as it courses superomedially. This raised rugosity probably represents a pronounced temporal line, though damage to the area renders such a conclusion tentative. However, such a clear distinction between the temporal line and the superior nuchal line would be inconsistent with the presence of a compound temporal/nuchal (T/N) crest. The relatively low positioning of the superior nuchal line on SKW 18 supports such a suggestion. The supramastoid crest and the mastoid crest of SK 52 are separated by a shallow groove ca. 8.0 wide; this supramastoid sulcus broadens slightly as the supramastoid and mastoid crests diverge toward the posterior. Thus we judge that there is no indication that a compound T/N crest is present in SKW 18/SK 52. As a result of the configuration of the temporal and nuchal crests, the "bare area" of Dart (1948) is moderately large in this specimen.

Relative to the size of the basicranium, the occipital condyles appear small (right: 18.0 anteroposterior (AP), 10.6 mediolateral (ML); left: 17.8 AP, 10.5 ML). They are anteriorly convergent, and the articular surfaces are directed anteriorly, inferiorly, and notably laterally, with a distinct ventral angulation. The condyles are oval-shaped, with small, diamond-shaped depressions visible on the anteromedial face. A single hypoglossal canal is found on each side externally (right, 3.9×5.1 ; left, 3.0×5.6), while internally the right side divides into a smaller, secondary canal. Immediately posterolateral to the occipital condyles is a moderately deep condylar fossa; small condylar canals are evident. Lateral to the condyles, large, robust jugular processes are present, each of which exhibits a distinct, inferiorly-directed, V-shaped paramastoid process. Immediately posterior to the paramastoid process is a roughened elevation for the insertion of *m. rectus capitis lateralis*.

Approximately 7.2 anterior to the anterior border of the foramen magnum (basion), moderately pronounced ridges are evident bilaterally, coursing roughly mediolaterally. A further 4.2 anterior to these ridges are two additional elongated, slightly more anteromedially directed elevations. These ridges combine to partially enclose a large, oval fossa marking the bony insertion of the *m. longus capitis*. They are deficient laterally, as there is no contact between the ridges at the lateral edges of the basiocciput. This has the effect of producing a "doubled" appearance to the *m. longus capitis* tubercles. The total area occupied by *m. longus capitis* is estimated at approximately 15.0×9.0 . Immediately pos-

terior to the posterior-most ridges are moderately excavated fissures, which are in turn positioned immediately anterior to the occipital condyles, corresponding to the insertion of *m. rectus capitis anterior*. In the midline, approximately 8.9 anterior to basion, is the well-developed pharyngeal tubercle. The sphenoccipital synchondrosis is unfused on both the internal and external aspects of the cranium. The meeting of the sphenoid and the occipital occurs about 22.5 anterior to basion.

Most of the right mastoid process was sheared off laterally (represented on SK 52), exposing extensive pneumatization. The left mastoid of SKW 18 is intact, with two oblique cracks on the posterolateral and inferolateral faces, respectively. When SK 52 is refit to SKW 18, both mastoids appear large and well-developed, projecting both inferiorly and laterally with a bulbous lateral contour when viewed from the posterior aspect. They represent the most lateral points on the cranial base, being inflated beyond the lateral extent of the supramastoid crest. There is a moderate anterior tilt of the mastoid, with the posterolateral face presenting a more oblique angle than the nearly vertical inferolateral face. The mastoids do not project inferiorly beyond the level of the occipital condyles, instead falling approximately 0.5 short of the plane of the condyles. The mastoid tips are located very close behind porion. The medial face of the left mastoid process slopes steeply into a deep, V-shaped mastoid notch. The small (15.0×6.0) mastoid notch traverses obliquely anteriorly toward a small stylo-mastoid foramen between the mastoid and tympanic, immediately lateral to the jugular process. The right mastoid was removed, but the unfused occipitomastoid suture is visible, beginning at the lateral root of the jugular process. The remnant of the right mastoid region in SKW 18 was superiorly displaced relative to the occipital along the length of the occipitomastoid suture. The left occipitomastoid suture is visible anteriorly, beginning at the root of the jugular process, approximately medial to the stylo-mastoid foramen. It courses posteriorly around the mastoid region, and curves upward along the nuchal plane until its extent is obscured by damage. A moderately developed occipitomastoid crest is present bilaterally, traversed by the occipitomastoid suture. Lateral to the occipitomastoid crest is a narrow channel for the occipital artery. Between the channel for the occipital artery and the mastoid notch is a well-developed juxtamastoid eminence, which is more inferiorly projecting than the occipitomastoid crest.

The right tympanic was obliquely sheared off, and thus lacks the lateral half (represented on SK 52). The left tympanic is complete from the meatus until just anterior to the jugular process. The lateral margin of the left tympanic is overhung by a moderately well-developed supramastoid crest, with the superior margin of the meatus itself some 3.7 medial to the lateral extent of the crest. The tympanic is oriented almost vertically, with a distinctly anteriorly inclined inferior face. It appears long and straight, with only a slight ML concavity. At its lateral extent, the tympanic flares moderately to form a cone-shaped structure. The petrous crest is relatively sharpened along its entire length. A distinct fissure delineates the tympanic from the mastoid, which Tobias (1991) referred to as the tympanomastoid fissure. Anteriorly, the petrotympanic fissure remains salient throughout its entire length. On the left side, medial to the stylo-mastoid foramen, is an area of damage which revealed what might be the root of an ossified styloid process. The lateral margin of the tympanic plate exhibits a thin infe-

rior floor, and a thicker anterosuperior portion, with the thickest part represented by the posteroinferior edge; the posterosuperior portion is deficient. The anterosuperior margin presents a "doubling-over," similar to that displayed by OH 5 (Tobias, 1967).

The right mandibular fossa was extensively damaged, while the left fossa is moderately well-preserved. The lateral extent of the left mandibular fossa was slightly abraded, the remainder being preserved medially to the entoglenoid process. Plastic deformation of the left pre-glenoid area produced a nearly vertical inclination of the posterior face of the articular tubercle, imparting an artificially narrow appearance to the fossa. The damage manifest on both mandibular fossae makes measurement unreliable, though it is clear that they were moderately deep, as seen in other *A. robustus* crania. A slight medio-lateral convexity is evident on the posterior face of the articular tubercle. The medial extent of the anterior wall of the mandibular fossa is notably recurved, and ends up facing more laterally than posteriorly. The entoglenoid process is particularly inferiorly prominent, angled at nearly 90° to the mandibular fossa ceiling. The entoglenoid is comprised in equal parts of a temporal squamosal portion, representing the medial extent of the mandibular fossa, abutting against an equally inferiorly projecting sphenoid component. The sphenosquamus suture bisects the entoglenoid into its squamosal and sphenoid portions. Immediately medial to the entoglenoid is a broad, deep channel separating the entoglenoid from the tympanic plate, the anteromedial recess of the mandibular fossa (Tobias, 1991). The postglenoid process is moderate-sized and flat, being closely applied to the doubled-over anterior surface of the tympanic plate; these structures merge superiorly to form the posterior wall of the mandibular fossa. The tympanic is laterally expanded beyond the lateral extent of the postglenoid. The lateral margin of the postglenoid process is nearly vertical, while the medial margin tapers superomedially, dividing the posterior wall of the mandibular fossa along a diagonal line. The inferomedial half of the posterior wall of the mandibular fossa is formed by the tympanic, while the superolateral half is comprised of the postglenoid process. Approximately 24.9 medial to the left meatal aperture, the basilar opening of the carotid canal is clearly visible, traversing anteromedially toward the internal carotid sulcus.

The foramen ovale is relatively small (left, 6.9 × 4.5; right, 6.6 × 4.1), and is encircled by the greater wing of the sphenoid. The lateral, posterior, and medial borders of the foramen are steep-sided, while the anterior border more gently grades into the inferior surface of the greater wing of the sphenoid. Approximately 2.2 lateral to the foramen ovale, the unfused sphenosquamus suture is visible on the right side, coursing anteriorly in a gently rounded arc from the anteromedial extent of the mandibular fossa for ca. 19.0 until its extent is obscured by damage. What remains of the pterygoid processes is relatively shortened, such that the medial and lateral pterygoid plates become salient closer to the basicranium than is seen in extant humans. Remnants of the left pterygoid plates bound what is judged to have been a moderate-sized pterygoid fossa. Around 4.0 superior to the posteromedial roots of the pterygoid processes, two small, comma-shaped foramina ramify medially into the body of the sphenoid, probably representing pharyngeal canals. Viewed laterally, the left lateral pterygoid plate is anteroposteriorly expanded, measuring 22.6 from its

posterior margin to its terminus at the spheno-maxillary fossa; it appears to be more posteriorly inclined than is typical of modern humans. The lateral face of the left lateral pterygoid is divided into two moderately deep, subequal circular depressions by a well-developed ridge running obliquely inferiorly. The anterosuperior depression is particularly deeply excavated, being overhung superiorly by a well-developed pterygoid ridge; it is occupied by a moderate-sized crack.

DISCUSSION

In their analysis of cranial base measures of primates and early hominids, Dean and Wood (1981, 1982) examined the only two specimens of *A. robustus* preserving sufficient cranial base morphology, TM 1517a and SK 47. The addition of SKW 18 expands the range of measures for this taxon (Table 1), probably owing to its status as a large male individual. In particular, SKW 18 appears as broad as, or broader than, TM 1517a and SK 47 in all measures, and longer in most measures except for tympanic plate (TP-CC) length and biforamen ovale to bitympanic line (FO/FO-TP/TP) length (Dean and Wood, 1981, 1982). Interestingly, values for the petrous and tympanic angles in SKW 18 fall between the two other *A. robustus* specimens, suggesting that these angles are not influenced by absolute size. Inclusion of SKW 18 in the *A. robustus* sample causes an overlap in bipetrous breadth with *A. africanus*, where previously *A. robustus* appeared narrower. The basioccipital length of *A. robustus* was formerly based on a single juvenile specimen, SK 47, presenting a remarkably short basioccipital. SKW 18 possesses a basioccipital which rivals that seen in *A. africanus*, *A. boisei*, and specimens of early *Homo*, resulting in overlapping values between these taxa.

SKW 18 retains certain elements of internal cranial anatomy which are not preserved in any other specimens of *A. robustus*. In Sts 5, OH 5, OH 24, and modern humans, the dorsum sellae is comprised of a thickened ridge of bone, and the posterior clinoid processes appear to be at least as broadly positioned as the dorsum sellae, if not broader. SKW 18, on the other hand, presents a thin, fragile dorsum sellae, with inwardly (medially) recessed posterior clinoid processes. The superior orbital fissures of SKW 18 match the fissure pattern that Rak et al. (1996) recognized in East African "robust" australopithecines and *Homo*, but which present as ape-like foramina in *A. afarensis* and *A. africanus*. The posterior edges of the lesser wings of the sphenoid are more bluntly rounded than is seen in humans, and they do not overhang the middle cranial fossa to the same extent. In this regard, SKW 18 is similar to specimens of *A. africanus* (Sts 5 and MLD 6) and *H. habilis* (OH 24). In Sts 5 and Sts 19, the carotid sulcus opens well below, and is clearly demarcated from, the floor of the sella turcica. In SKW 18 and OH 5, the carotid sulcus is not as distinctly segregated from the floor of the sella turcica. The carotid sulcus is positioned nearer to the tuberculum sellae in SKW 18, unlike other hominin crania where it makes a closer approach to the dorsum sellae.

SKW 18 shares a variety of anatomical characteristics with other specimens of *A. robustus* from Swartkrans and Kromdraai (Table 2). Yet owing to a paucity of cranial remains attributed to *A. robustus*, insufficient information regarding intraspecific variability in the cranial base of this taxon is available; inclusion of SKW 18 in the *A. robustus* sample provides additional details. The

TABLE 1. Cranial base measurements for *Australopithecus robustus*, including SKW 18¹

	Widths										Lengths				Angles		
	TP-TP	SP-SP	CC-CC	FO-FO	IT-IT	SM-SM	PA-PA	FM-FM	BS-OP	TP-CC	CC-PA	SB-BS	IV/IT-TP/TP	FO/FO-TP/TP	IT/IT-BS	Petrous	Tympanic
SK 47	100	68	51	43	54	78	22	20	27	25	20	12	45	23	37	45	107
TM 1517a	(118)	66	(50)	(41)	(61)	67	(18)			(35)	(21)		63	35	57	42	115
SKW 18	(120)	76	(54)	43	(26)	81	(26)	23	29	(28)	(22)	22	63	28		42	110

¹ See Dean and Wood (1981, 1982) for descriptions of measurements.

Linear measurements are recorded to nearest mm. Angles are recorded to nearest degree. Values in parentheses are either estimated lengths, or widths measured to midline and doubled.

TABLE 2. Morphological features of the cranial base that SKW 18 shares with other specimens of *A. robustus*

1. Superior petrosal border is well-rounded, and does not overhang posterior cranial fossa
2. Petrous part is coronally oriented
3. Internal occipital protuberance weakly developed and positioned low, close to opisthion
4. Inferior sagittal limb of cruciform eminence long, low, and broad
5. Small vermiform fossa evident
6. Venous sinus impressions on posterior cranial fossa in form of occipital/marginal system
7. Marked expansion of cerebellar impressions on posterior cranial fossa
8. Weakly inclined nuchal plane
9. Inion positioned low on occipital
10. External occipital protuberance strongly developed
11. External occipital crest strongly developed
12. Nuchal musculature moderately developed
13. Simple supramastoid crest originating from temporal line
14. Absence of compound T/N crest, and presence of concomitant moderate-sized "bare area"
15. Foramen magnum oriented downward and roughly horizontally
16. Oval-shaped (not cardioid) foramen lacking ectobasionic process or lateral embayments
17. Foramen magnum positioned well anterior to bitympanic line
18. Large, heavily pneumatized mastoid processes
19. Mastoids notably laterally inflated, representing most lateral points on cranial base
20. Mastoids tips slightly inflected beneath cranial base, positioned close to level of porion
21. Well-developed tympanomastoid groove separates mastoids from tympanic
22. Deep, narrow, V-shaped mastoid notch
23. Posteriorly extended mastoid notch isolates mastoid process from remainder of temporal
24. Pronounced juxtamastoid eminence indicated
25. Well-developed occipitomastoid crest confluent with occipitomastoid suture
26. Prominent paramastoid processes for articulation with atlas
27. External acoustic meatus distinctly laterally positioned
28. Cone-shaped tympanic
29. Tympanic plate nearly vertically inclined
30. Petrous crest well-developed
31. Mandibular fossa deep, with moderate articular eminence
32. Anteromedial recess of mandibular fossa (instead of medial recess)
33. Postglenoid process small and closely appressed to tympanic, with both structures merging superiorly
34. Posterior wall of mandibular fossa comprised of tympanic medially and postglenoid laterally
35. Strong attachment for pterygoid musculature

superior petrosal border of SKW 18 displays a similar morphology to some specimens of *A. robustus* (SK 1585 and DNH 7), in that the border appears gently rounded along its entire length. Other specimens (SK 46 and TM 1517a) exhibit a superior petrosal border that becomes sharper laterally, limiting the value of this feature in taxonomic diagnoses (see also Ahern, 1998; Lockwood and Tobias, 1999). Lockwood and Tobias (2002) discussed the potential utility of the shape of the opening for the vestibular aqueduct on the posterior petrosal surface for identifying isolated hominin temporal bones. SKW 18 possesses an opening formed as a right angle, while SK 46, the only other specimen from Swartkrans preserving this area, has an opening formed as a curved slit, limiting the applicability of this trait in *A. robustus*.

Tobias (1967) described an unusual pattern of cranial blood drainage in OH 5 and SK 859, which was later recognized in several crania attributed to *A. afarensis*, *A. robustus*, and *A. boisei* (Falk, 1986a,b; Falk and Conroy, 1983; White and Falk, 1999), as well as some specimens of *A. africanus* (Lockwood and Tobias, 2002; Tobias and Falk, 1988). Falk (1986b) suggested that this occipital/marginal (O/M) venous sinus pattern was fixed at 100% in specimens of *A. afarensis* and “robust” australopithecines, indicating a close phylogenetic link for these taxa. Kimbel (1984; see also Kimbel et al., 2004) maintained that this pattern was evident in only 8 of 9 (89%) *A. afarensis* crania, and that some modern human populations are characterized by high frequencies of this trait (see also Browning, 1953; Das and Hassan, 1970; Woodhall, 1936), limiting its phylogenetic valence. SKW 18 displays an O/M system, and thus this feature is recorded in 100% (3 out of 3) of *A. robustus* crania preserving this area. However, while the O/M pattern is expressed strongly in SK 859 and to a lesser extent in SK 1585, it is only faintly palpable in SKW 18, indicating significant intraspecific variability. Strong O/M systems are present in both large (OH 5) and small (SK 859) individual “robust” australopithecines, while weak expression can be found in large individuals (SKW 18), indicating that expression of this trait is unlikely to be a result of size dimorphism. Although a detectable O/M system is present in all three relevant specimens of *A. robustus*, the expression of the marginal sinus groove is variable, ranging from bilaterally present (SK 859), to unilaterally present (SK 1585), to bilaterally undetectable (SKW 18). If substantial marginal sinuses were present in SKW 18, they most likely drained into the larger sigmoid sinus, unlike the condition in OH5, where the sigmoid sinus appears to have been the contributory vessel, emptying into the larger marginal sinus prior to exiting via the jugular (Tobias, 1967).

Tobias and Symons (1992) hypothesized that *A. robustus* might be characterized by a cardioid foramen magnum similar to that seen in *A. boisei* (Tobias, 1967) and perhaps *A. aethiopicus* (Walker et al., 1986), thus forming a unique synapomorphic character complex in the “robust” australopithecine lineage. They suggested that this unusual shape might be a by-product of the expanded development of the O/M venous sinuses as they drained via the foramen magnum into the vertebral plexus of veins. With its oval-shaped foramen magnum lacking an ectobasionic projection or lateral embayments, SKW 18 does not conform to the pattern proposed by Tobias and Symons (1992). The oval-shaped foramen magnum of SK 47, the only other representative of *A. robustus* retaining a relatively complete foramen magnum, is similar to SKW 18, demonstrating no indication of a cardioid foramen magnum in this taxon. This in turn suggests that cranial blood flow via the foramen magnum into the vertebral plexus was not as significant in *A. robustus* as in East African “robust” australopithecines.

The pronounced development of the external occipital protuberance as a marked ridge in SKW 18 indicates considerable variability in this structure, possibly relating to the status of SKW 18 as a large male. This ridge-like protuberance results in inion being positioned relatively low on the occipital, separating it more widely from lambda than is indicated in other specimens of *A. robustus*. The lack of a compound T/N crest, and concomitant presence of a moderate-sized “bare area” in SKW 18, is in broad agreement with other specimens of

A. robustus. Since SKW 18 is a large male, this would indicate that *A. robustus* can be characterized by the lack of a compound T/N crest (Robinson, 1958; contra Tobias, 1967). The tympanic of *A. robustus* is not as distinctly cone-shaped in SKW 18 as in specimens such as SK 46, SK 848, and SKW 2581. The occipital condyles in SKW 18 are broader than is seen in other specimens of *A. robustus*. The anterosuperior corner of the external acoustic meatus is “doubled over,” unlike other *A. robustus* crania, although SK 46 shows a distinct thickening of the area that almost presents as a “doubled” meatus. The inferiorly oriented entoglenoid process of SKW 18 is comprised of equal parts squamosal and sphenoid, whereas in other specimens of *A. robustus*, the entoglenoid is comprised mostly of squamosal bone, with minimal contribution from the sphenoid.

The *m. longus capitis* tubercles of *A. africanus* are anteroposteriorly directed and appear as enclosed bilateral basins (Lockwood and Tobias, 2002, p. 417). In SKW 18, the *m. longus capitis* basins are more mediolaterally oriented and bounded anteriorly and posteriorly, but not laterally, by distinct bony tubercles, thus presenting a “doubled” appearance (Fig. 2b). Other, smaller specimens of *A. robustus* such as SK 47 (juvenile) and SK 48 (female?) do not exhibit the pronounced prevertebral muscular insertions seen in SKW 18. Dean (1985) hypothesized that in both “gracile” and “robust” australopithecines, *m. longus capitis* might be the only powerful flexor of the cranium, resulting from the poor development of the mastoids (indicating weaker development of sternocleidomastoideus) as well as their position behind the axis of rotation of the occipital condyles. At the same time, the counterbalance effect of the massive face of “robust” australopithecines reduced the need for powerfully developed *m. longus capitis* muscles, thus accounting for the weak development of the tubercles in *A. robustus* vs. *A. africanus*. The mastoid processes of SKW 18 are large and well-developed, and are positioned very close to the condylar axis of rotation, leaving them as strong cranial flexors. The *m. longus capitis* insertions are also powerfully developed, despite the fact that SK 52 presents substantial facial architecture. This suggests that size dimorphism played a significant role in the development of the prevertebral muscular insertions in *A. robustus*, and that both *m. longus capitis* and *m. sternocleidomastoideus* served as important cranial flexors.

Olson (1978) suggested that SK 47 most likely represented early *Homo* and not *A. robustus*, as previously concluded (Broom and Robinson, 1952; Robinson, 1956). This suggestion was based in part on a confusion of the occipitomastoid crest and juxtamastoid eminence, as recognized in subsequent publications (Kimbel et al., 1985; McKee and Helman, 1991; Olson, 1985). Nonetheless, Olson (1985, p. 108) argued that no “robust” australopithecine specimens exhibited a juxtamastoid eminence or occipitomastoid crest, concluding that a juxtamastoid eminence had not evolved in the “robust” australopithecine clade, while the occipitomastoid crest was incorporated into the medial wall of the mastoid process. Others (Kimbel et al., 1985, 2004; McKee and Helman, 1991) recognized the presence of a distinct occipitomastoid crest and juxtamastoid eminence in the Swartkrans sample, particularly in SK 47. SKW 18 possesses a well-developed occipitomastoid crest and juxtamastoid eminence that differ only slightly from the configuration in SK 47, in that these two structures merge posteriorly in SK 47, but not in SKW 18. SKW 18 also possesses a

more powerfully developed juxtamastoid process that overshadows the occipitomastoid crest. The similar occipitomastoid-region anatomy in SKW 18 and SK 47, and indeed in all *A. robustus* specimens in South Africa (McKee and Helman, 1991), alongside considerable dental evidence (Robinson, 1956), argues against a designation of *Homo* for SK 47. The variability evident in this region across a variety of hominin specimens also argues against the presence of a unique anatomical link in the occipitomastoid region between “robust” australopithecines and certain cranial specimens from Hadar (contra Olson, 1981, 1985), in agreement with previous suggestions (Kimbel et al., 1985, 2004; McKee and Helman, 1991).

CONCLUSIONS

SKW 18 shares a number of morphological traits in the cranial base that clearly align it with *A. robustus*. At the same time, the expanded cranial base hypodigm of *A. robustus* is characterized by a notable degree of polymorphism, despite a limited number of relevant specimens. Variability in the expression of some traits in this anatomically conservative region, such as the development of the O/M system, does not appear to be linked to size dimorphism. Nevertheless, sexual dimorphism is evident in that males are characterized by large, inflated mastoids; well-developed nuchal muscle attachments, including pronounced external occipital protuberance development; and prominent development of the prevertebral musculature. No specimen of *A. robustus* presents a compound T/N crest, not even large males (e.g., SK 49 and SKW 18). The presence of an O/M system in SKW 18 confirms the fixity of this trait in *A. robustus*, though the lack of a cardioid foramen magnum differentiates this character complex from that evinced by *A. boisei*.

ACKNOWLEDGMENTS

We thank Francis Thackeray, Heidi Fourie, and Stephy Potze of the Transvaal Museum for permission to prepare and study this fossil, and for assistance with the comparative fossil material in their care. Bob Brain provided not only SKW 18 itself, but also exceptional support and insights into the complexities of Swartkrans. We thank Phillip Tobias for generously donating his time to examine this specimen, and for discussion of the anatomical minutiae preserved therein. Earlier drafts of this paper were significantly improved thanks to insightful commentary from Steve Churchill and two anonymous reviewers.

LITERATURE CITED

- Ahern JCM. 1998. Underestimating intraspecific variation: the problem with excluding Sts 19 from *Australopithecus africanus*. *Am J Phys Anthropol* 105:461–480.
- Berger LR, de Ruiter DJ, Steininger C. 2003. Preliminary results of excavations at the newly investigated locality Coopers D, Gauteng, South Africa. *S Afr J Sci* 99:276–278.
- Brain CK. 1981. *The hunters or the hunted?* Chicago: University of Chicago Press.
- Brain CK. 1993. Structure and stratigraphy of the Swartkrans cave in the light of new excavations. In: Brain CK, editor. *Swartkrans: a cave's chronicle of early man*. Transvaal Museum monograph no. 8. Pretoria: Transvaal Museum. p 7–22.
- Broom R. 1938. The Pleistocene anthropoid apes of South Africa. *Nature* 142:377–379.
- Broom R. 1949. Another new type of fossil ape-man. *Nature* 163:57.
- Broom R, Robinson JT. 1952. Swartkrans ape-man *Paranthropus crassidens*. Transvaal Museum memoir no. 6. Pretoria: Transvaal Museum.
- Browning H. 1953. The confluence of dural venous sinuses. *Am J Anat* 93:307–329.
- Clarke RJ. 1977. The cranium of the Swartkrans hominid SK 847 and its relevance to human origins. Unpublished Ph.D. dissertation, University of the Witwatersrand, Johannesburg.
- Conroy GC, Kuykendall K. 1995. Paleopediatrics: or when did human infants really become human? *Am J Phys Anthropol* 98:121–132.
- Curnoe D, Grun G, Taylor L, Thackeray JF. 2001. Direct ESR dating of a Pliocene hominin from Swartkrans. *J Hum Evol* 40:379–391.
- Dart RA. 1948. The Makapansgat proto-human *Australopithecus prometheus*. *Am J Phys Anthropol* 6:259–284.
- Das AC, Hassan M. 1970. The occipital sinus. *J Neurosurg* 33:307–311.
- Dean MC. 1985. Comparative myology of the hominoid cranial base II: the muscles of the prevertebral and upper pharyngeal region. *Folia Primatol (Basel)* 44:40–51.
- Dean MC, Wood BA. 1981. Metrical analysis of the basicranium of extant hominids and *Australopithecus*. *Am J Phys Anthropol* 54:63–71.
- Dean MC, Wood BA. 1982. Basicranial anatomy of Plio-Pleistocene hominids from East and South Africa. *Am J Phys Anthropol* 59:157–174.
- de Ruiter DJ. 2003. Revised faunal lists of Members 1–3 of Swartkrans, South Africa. *Ann Transvaal Mus* 40:29–41.
- Falk D. 1986a. Evolution of cranial blood drainage in hominids: enlarged occipital/marginal sinuses and emissary foramina. *Am J Phys Anthropol* 70:311–324.
- Falk D. 1986b. Endocast morphology of Hadar hominid AL 162–28: reply to Holloway and Kimbel. *Nature* 321:536–537.
- Falk D, Conroy GC. 1983. The cranial venous sinus system in *Australopithecus afarensis*. *Nature* 306:779–781.
- Federative Committee on Anatomical Terminology. 1998. *Terminologia anatomica*. New York: Thieme.
- Grine FE. 1993. Description and preliminary analysis of new hominid cranio-dental fossils from the Swartkrans formation. In: Brain CK, editor. *Swartkrans: a cave's chronicle of early man*. Pretoria: Transvaal Museum. p 75–116.
- Grine FE, Strait DS. 1994. New hominid fossils from Member 1 “Hanging Remnant,” Swartkrans Formation, South Africa. *J Hum Evol* 26:57–75.
- Keyser AW. 2000. The Drimolen skull: the most complete australopithecine cranium and mandible to date. *S Afr J Sci* 96:189–192.
- Keyser AW, Menter CG, Moggi-Cecchi J, Pickering TR, Berger LR. 2000. Drimolen: a new hominid-bearing site in Gauteng, South Africa. *S Afr J Sci* 96:193–197.
- Kimbel WH. 1984. Variation in the pattern of cranial venous sinuses and hominid phylogeny. *Am J Phys Anthropol* 63: 243–263.
- Kimbel WH, White TD, Johanson DC. 1985. Craniodental morphology of the hominids from Hadar and Laetoli: evidence of “*Paranthropus*” and *Homo* in the mid-Pliocene of eastern Africa? In: Delson E, editor. *Ancestors: the hard evidence*. New York: Alan R. Liss. p 120–137.
- Kimbel WK, Rak Y, Johanson DC. 2004. The skull of *Australopithecus afarensis*. Oxford: Oxford University Press.
- Krogman WM, Işcan MY. 1986. *The human skeleton in forensic medicine*. 2nd ed. Springfield, IL: C.C. Thomas.
- Kuman K, Clarke RJ. 2000. Stratigraphy, artefact industries and hominid associations for Sterkfontein, Member 5. *J Hum Evol* 38:827–847.
- Lockwood CA, Tobias PV. 1999. A large male hominin cranium from Sterkfontein, South Africa, and the status of *Australopithecus africanus*. *J Hum Evol* 36:637–685.
- Lockwood CA, Tobias PV. 2002. Morphology and affinities of new hominin cranial remains from Member 4 of the Sterkfontein formation, Gauteng province, South Africa. *J Hum Evol* 42:389–450.

- Mann AE. 1975. Some paleodemographic aspects of the South African australopithecines. *Univ Penn Publ Anthropol* 1:1-171.
- McKee JK, Helman SB. 1991. Variability of the hominid juxtastoid eminence and associated basicranial features. *J Hum Evol* 21:275-281.
- Menter CG, Kuykendall KL, Keyser AW, Conroy GC. 1999. First record of hominid teeth from the Plio-Pleistocene site of Gondolin, South Africa. *J Hum Evol* 37:299-307.
- Oakley KP. 1977. *Catalogue of fossil hominids*. London: British Museum (Natural History).
- Olson TR. 1978. Hominid phylogenetics and the existence of *Homo* in Member 1 of the Swartkrans formation, South Africa. *J Hum Evol* 7:159-178.
- Olson TR. 1981. Basicranial morphology of the extant hominoids and Pliocene hominids: the new material from the Hadar formation, Ethiopia, and its significance in early human evolution and taxonomy. In: Stringer CB, editor. *Aspects of human evolution*. London: Taylor and Francis, Ltd. p 99-128.
- Olson TR. 1985. Cranial morphology and systematics of the Hadar formation hominids and "*Australopithecus*" *africanus*. In: Delson E, editor. *Ancestors: the hard evidence*. New York: Alan R. Liss. p 102-119.
- Rak Y, Clarke RJ. 1979. Aspects of the middle and external ear of early South African hominids. *Am J Phys Anthropol* 51:471-474.
- Rak Y, Kimbel WH, Johanson DC. 1996. The crescent of foramina in *Australopithecus afarensis* and other early hominids. *Am J Phys Anthropol* 101:93-99.
- Robinson JT. 1956. *The dentition of the Australopithecinae*. Transvaal Museum memoir no. 9. Pretoria: Transvaal Museum.
- Robinson JT. 1958. Cranial cresting patterns and their significance in the Hominoidea. *Am J Phys Anthropol* 16:397-428.
- Tobias PV. 1967. The cranium of *Australopithecus (Zinjanthropus) boisei*. Olduvai Gorge volume 2. Cambridge: Cambridge University Press.
- Tobias PV. 1991. The skulls, endocrasts and teeth of *Homo habilis*. Olduvai Gorge volume 4. Cambridge: Cambridge University Press.
- Tobias PV, Falk D. 1988. Evidence for a dual pattern of cranial venous sinuses on the endocranial cast of Taung (*Australopithecus africanus*). *Am J Phys Anthropol* 76:309-312.
- Tobias PV, Symons JA. 1992. Functional, morphogenetic and phylogenetic significance of conjunction between foramen magnum and enlarged occipital and marginal venous sinuses. *Archaeol Oceania* 27:143-152.
- Ubelaker DH. 1989. *Human skeletal remains: excavation, analysis, interpretation*. 2nd ed. Washington, DC: Taraxacum.
- Vrba ES. 1985. Early hominids in southern Africa: updated observations on chronological and ecological background. In: Tobias PV, editor. *Hominid evolution: past, present and future*. New York: Alan R. Liss. p 195-200.
- Walker A, Leakey REF, Harris JM, Brown FH. 1986. 2.5-Myr *Australopithecus boisei* from west of Lake Turkana, Kenya. *Nature* 322:517-522.
- Weidenreich F. 1943. The skull of *Sinanthropus pekinensis*: a comparative study on a primitive hominid skull. *Palaeontol Sin* 10:1-485.
- White DD, Falk D. 1999. A quantitative and qualitative reanalysis of the endocrast from the juvenile *Paranthropus* specimen L338y-6 from Omo, Ethiopia. *Am J Phys Anthropol* 110:399-406.
- Woodhall B. 1936. Variations of the cranial venous sinuses in the region of the torcular herophili. *Arch Surg* 33:297-314.